Microelectronics Reliability 64 (2016) 434–439

Contents lists available at ScienceDirect

Microelectronics Reliability

journal homepage: www.elsevier.com/locate/microrel

Development and characterisation of pressed packaging solutions for high-temperature high-reliability SiC power modules

J. Ortiz Gonzalez [a,*], A.M. Aliyu [b], O. Alatise [a], A. Castellazzi [b], L. Ran [a], P. Mawby [a]

[a] School of Engineering, University of Warwick, Coventry, United Kingdom
[b] Power Electronics, Machines and Control Group, University of Nottingham, Nottingham, United Kingdom

ARTICLE INFO

Article history:
Received 29 June 2016
Accepted 8 July 2016
Available online 18 September 2016

Keywords:
SiC
Aluminium graphite
Pressure packaging

ABSTRACT

SiC is a wide bandgap semiconductor with better electrothermal properties than silicon, including higher temperature of operation, higher breakdown voltage, lower losses and the ability to switch at higher frequencies. However, the power cycling performance of SiC devices in traditional silicon packaging systems is in need of further investigation since initial studies have shown reduced reliability. These traditional packaging systems have been developed for silicon, a semiconductor with different electrothermal and thermomechanical properties from SiC, hence the stresses on the different components of the package will change. Pressure packages, a packaging alternative where the weak elements of the traditional systems like wirebonds are removed, have demonstrated enhanced reliability for silicon devices however, there has not been much investigation on the performance of SiC devices in press-pack assemblies. This will be important for high power applications where reliability is critical. In this paper, SiC Schottky diodes in pressure packages have been evaluated, including the electrothermal characterisation for different clamping forces and contact materials, the thermal impedance evaluation and initial thermal cycling studies, focusing on the use of aluminium graphite as contact material.

1. Introduction

Power device packaging involves intimate contact between different materials with different thermomechanical properties. Coefficient of Thermal Expansion (CTE) mismatch between the semiconductor, the die attach and the baseplate causes thermomechanical stresses which increase the thermal resistance and junction temperature of the device under power cycling. The wirebond to source/gate metal interface is another reliability concern due to the occurrence of wirebond lift-off. Current packaging systems have been developed for silicon rather than silicon carbide hence, the different thermomechanical properties of SiC lead to different stresses on the elements of the packaging system. This results in a reduced power cycling capability of the current SiC devices compared with their silicon counterparts [1].

A packaging alternative where the elements of the packaging subjected to thermomechanical stresses are removed, achieving an enhanced reliability, is the press-pack modules [2]. Press-pack modules also improve the system fault tolerance by failing to short. Press-pack modules have typically been used in high power applications like HVDC line-commutated converters where series connected thyristors are required for high DC voltage blocking capability. Press-pack IGBTs have been demonstrated by ABB and IXYS. Hence, voltage source converter technology in press-pack is possible. In a press-pack module, the semiconductor is pressed between two copper heatsinks/electrodes, using an intermediate thermal contact to match the CTE. The weak elements of the packaging system (solder and wire bonds) are removed thus achieving enhanced reliability, despite the more complex assembly system. There are few studies on the implementation of SiC in press-pack [3,4], however, the availability of larger SiC dies and the limited reliability shown by the traditional packaging systems suggest that SiC press-pack modules could be a suitable alternative, particularly considering the enhanced power cycling capability demonstrated in [4]. A prototype for the evaluation of a SiC Schottky diode in pressure packages is presented in Section 2. Here, aluminium graphite as an alternative contact material to molybdenum and DC heating measurements are presented. The thermal impedance of this packaging system, considering different forces and different contact materials, is evaluated in Section 3 with initial power cycling results presented in Section 4. Section 5 concludes the paper.

2. Prototype for the evaluation of silicon carbide devices in press-pack

A prototype for the evaluation of a single 1200 V/50 A SiC Schottky diode (CPW5-1200-Z050B from Wolfspeed) on press-pack has been developed and it is shown in Figs. 1 and 2. A die carrier made of PPS is used for positioning the die and the intermediate contacts used for matching

* Corresponding author.
E-mail address: J.A.Ortiz-Gonzalez@warwick.ac.uk (J. Ortiz Gonzalez).

http://dx.doi.org/10.1016/j.microrel.2016.07.062
0026-2714/

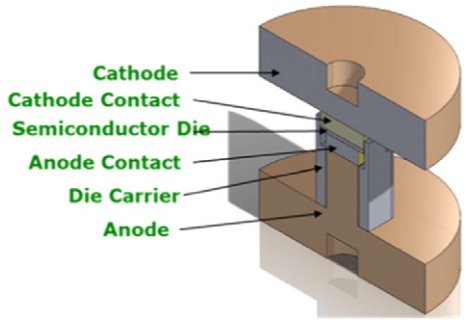

Fig. 1. Cross-section of the prototype.

the CTE of the semiconductor. An external case made of PEEK is used for aligning the copper poles. PPS and PEEK are both engineering plastics, dimensionally stable with a temperature of operation over 200 °C. The evaluated prototype is not hermetic, hence the maximum operating voltage would be limited.

The size of the CPW5-1200-Z050B Schottky diode die is 4.9 mm × 4.9 mm with a thickness of 380 μm. The dimensions of the intermediate contacts are 3.7 mm by 3.7 mm for the anode contact and 4.9 mm by 4.9 mm for the cathode contact. The intermediate contacts have a thickness of 1.5 mm and have been machined with a radius of 0.5 mm, with a pressed area of 13.48 mm^2 and 23.80 mm^2. According to [2], the usual clamping force for optimal electrical and thermal contact ranges from 10 to 20 N/mm^2 and for the studies on a single chip presented on this paper clamping forces of 300 N and 500 N have been selected.

The traditional material for the intermediate contacts is molybdenum, but aluminium graphite (ALG), a metal matrix composite by Schunk Hoffmann [5], appears as a suitable alternative. The properties of ALG2208, anisotropic material, compared with molybdenum and silicon carbide [1,5,6] are shown in Table 1.

With a suitable CTE and a high thermal conductivity [5], the electro-thermal performance of this alternative material is going to be evaluated in this paper. A picture of the ALG contact, where the aluminium and graphite structure is easily identified, is represented in Fig. 3.

2.1. Analysis of the electrical and thermal characteristics using pressure contacts

A simplified electrical model of the press-pack diode is represented in Fig. 4 and the thermal model can be represented using a basic Cauer network, as it has been done in [7] for a press-pack IGBT module.

Table 1
Properties of ALG2208, molybdenum and SiC.

	ALG2208	Mo	SiC
Thermal conductivity (W/m °C)	x,y: 220 z: 140	138	380
Thermal capacity (J/kg °C)	800	217	690
Density (kg/m^3)	2300	10,220	3210
CTE (μm/m °C)	x,y: 8 z: 12	5.35	4.3
Resistivity (Ω/m)	x,y: $4e^{-7}$ z: $6e^{-7}$	$5.3e^{-8}$	–

The electrical resistance of a conductor is determined by Eq. (1), where ρ is the resistivity of the material, d the thickness and A the cross section of the material.

$$R = \rho \frac{d}{A} \tag{1}$$

The electrical contact resistance can be determined using the Eq. (2) [6].

$$R_{Contact1-2} = \frac{\rho_1 + \rho_2}{4} \sqrt{\frac{\pi H}{F}} \tag{2}$$

where ρ_1 and ρ_2 are the resistivity of the materials in contact, H the hardness of the softer material and F the applied force. The thermal resistances and capacitances are determined by Eqs. (3) and (4), where d is the thickness of the material, A the cross section of the material, λ_{th} the thermal conductivity, c_{heat} the thermal capacity and ρ the density of the material.

$$R_{TH} = \frac{d}{\lambda_{th} A} \tag{3}$$

$$C_{TH} = c_{heat} \rho dA \tag{4}$$

The thermal contact conductance, assuming negligible radiation heat transfer [6,8] is determined by Eq. (5), where k_s is the mean thermal conductivity, σ the effective root mean square of surface roughness, m the mean absolute surface flatness, P the contact pressure and H_C the contact microhardness.

$$h_c = 1.25 k_s \frac{m}{\sigma} \left(\frac{P}{H_C} \right)^{0.95} \tag{5}$$

These equations show the impact of the roughness and flatness of the surfaces in contact on the electrical and thermal contact [4]. For

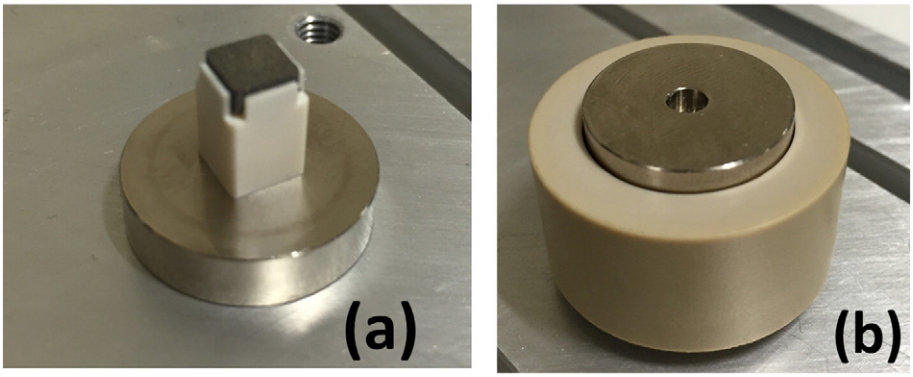

Fig. 2. Assembly of the prototype (a) without the external case (b) with the external case.

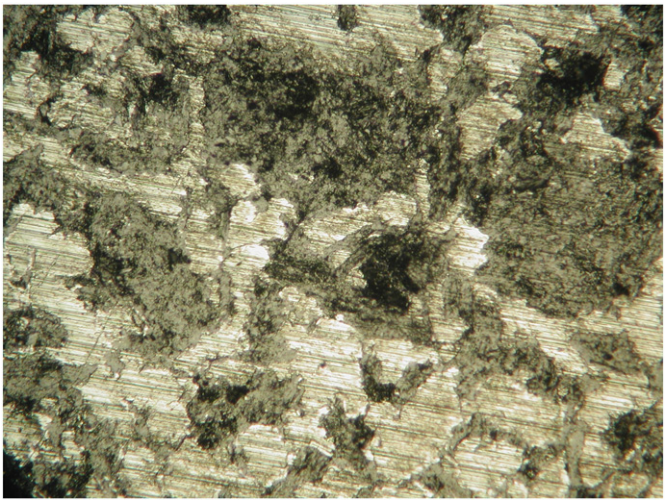

Fig. 3. Surface of the ALG contact.

this study the contacts have not been plated, hence the surface characterisation of the non-plated molybdenum and ALG contacts is shown in Figs. 5 and 6. The average surface roughness S_A is 0.763 μm for the molybdenum contacts and 0.736 μm for the ALG contacts. Despite having a similar average surface roughness, in Fig. 6 the effect of the different materials composing the ALG structure can be observed.

2.2. Initial measurements and considerations

The initial evaluation of the electrothermal properties of the press-pack diode has been done using a traditional DC power cycling test set-up where the calibrated forward voltage at low currents is used for estimating the junction temperature [9]. Box clamps BX-42, rated at 300 N and 500 N, and a heatsink model PS260/150B, both from GD Rectifiers, are used for these DC heating tests.

Fig. 7 shows the forward voltage at high current during the heating of the diode, where the effect of the contact material on the forward voltage can be seen. ALG has a higher resistivity, hence the forward voltage is higher when ALG contacts are used.

The effect of the clamping force on the forward voltage using ALG as contact is presented on Fig. 8. According to Eq. (2) and the schematic shown in Fig. 4, increasing the clamping force reduces the contact resistance, hence it reduces the voltage drop across the press-pack diode. For a heating current of 30 A the slope of the voltage during the heating has reduced slightly, suggesting a higher thermal conductivity when the clamping force is increased, as Eq. (5) indicates.

The thermal response for ALG and molybdenum contacts for different DC heating currents and a clamping force of 500 N is shown in Fig. 9.

3. Thermal impedance characterisation

The transient thermal response shown in Fig. 9 is caused by the different thermal impedance of the ALG and molybdenum contacts, as the

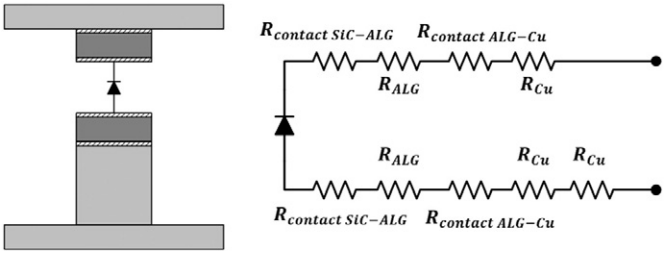

Fig. 4. Equivalent electrical model of the press-pack diode.

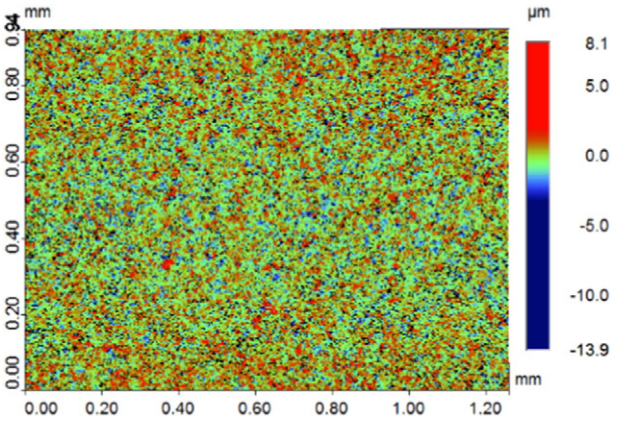

Fig. 5. Surface roughness of the molybdenum contact.

measurements and the analytical equations on Section 2 show. The impact of the contact material and the clamping force is going to be evaluated in this section using a dedicated thermal impedance characterisation equipment that is capable of performing power cycling and reliability evaluation on a module by extracting the impact of thermomechanical stresses on the transient thermal impedance of the module [10].

The thermal impedance which is a function of the thermal transient can be transformed into a graphical representation of the structure called the structure function [11]. The structure functions are obtained by direct mathematical transformations from the heating or cooling curves [12]. The structure function uses the thermal resistances and capacitances in the Cauer form (because Cauer networks have a link with the physical structure) to identify changes in the structure of the device. There are two types of the structure function, differential and cumulative structure function. In [13] the differential structure function $K(R_\Sigma)$ is defined as the derivative of the cumulative thermal capacitance with respect to the cumulative thermal resistance.

$$K(R_\Sigma) = \frac{dC_\Sigma}{dR_\Sigma} \tag{6}$$

The differential structure function is used in Fig. 10 to analyze the two contacts at the same clamping force (500 N). The x-axis is the cumulative thermal resistance and the y-axis a function of the cumulative thermal capacitance. To help understand the relationship between Fig. 10 and the physical structure, an analytical calculation using Eq. (3) was carried out to get an approximate resistance of the die and the contact. In the differential structure function the local peaks indicate a new interface in the heat flow path, hence from the location of the peaks and

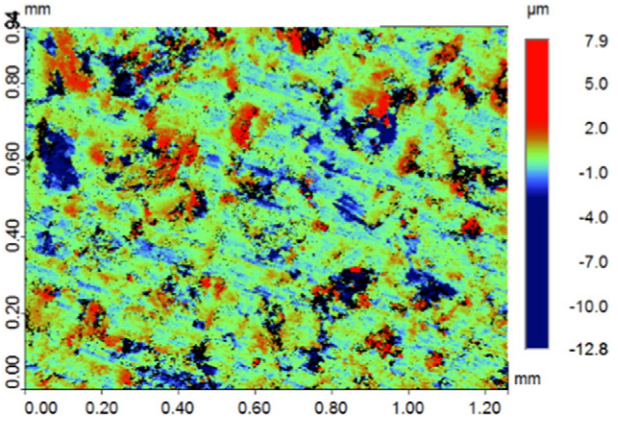

Fig. 6. Surface roughness of the ALG contact.

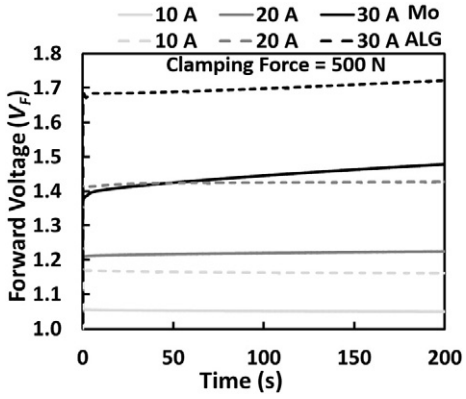

Fig. 7. Forward voltage during heating for different contact materials. Clamping force $F =$ 500 N.

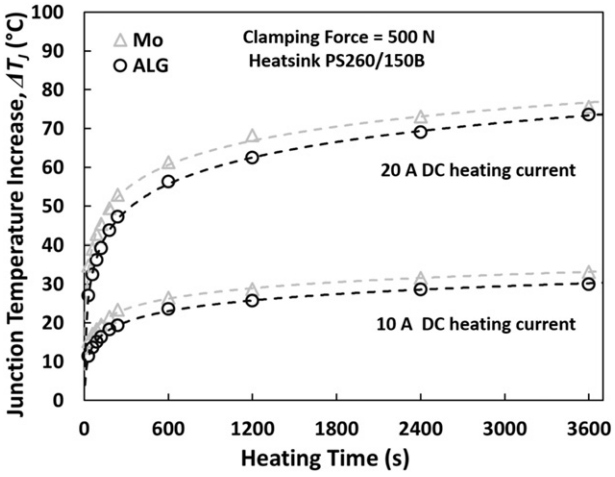

Fig. 9. Junction temperature during heating. ALG and Mo as intermediate contacts, clamping force of 500 N.

the analytical values shown in Table 2 the relationship between the structure and Fig. 10 has been deduced.

In Fig. 10 it can be observed that the die region for both ALG and molybdenum is the same, as the same force and the same die are used. An increased thermal resistance in molybdenum is observed after the die region. The total difference between the two contacts is a thermal resistance of 0.339 K/W. This means that for the same power an assembly with ALG will run at lower temperature. This gives ALG an advantage of high power density. For the same material (ALG), different clamping forces were implemented and the differential structure function measured. From Fig. 11 it can be seen that 500 N gives a better thermal performance as the different materials are in better contact.

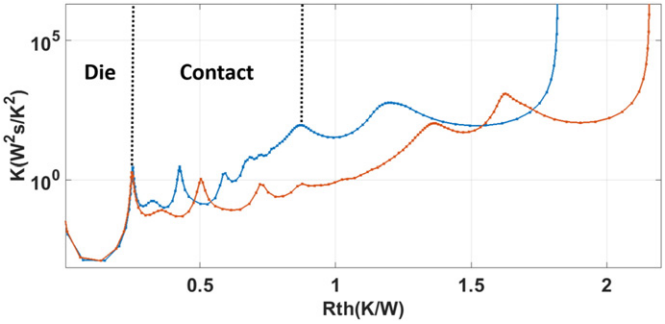

Fig. 10. Differential structure for ALG (blue) and molybdenum (red) at the same clamping force ($F =$ 500 N).

4. Power cycling results

The press pack was put under power cycling using constant current of 30 A to produce a change in the junction temperature during cycling (ΔT_J) of about 70 °C with a period of 60 s and a duty cycle of 0.5 [9]. One of the determinants of the number of cycles is the ΔT_J, as the number of cycles to failure is indirectly proportional to the ΔT_J. The maximum junction temperature (T_{Jmax}) for this test is 90 °C and the minimum (T_{Jmin}) is 16 °C. Fig. 12 shows the maximum junction temperature, the delta T and the minimum junction temperature.

In Fig. 12 repetitive spikes can be observed. This is due to the fact that after every two hundred cycles the thermal impedance of the device is measured and transformed into the cumulative structure function and the differential structure function. The cumulative structure function is sum of the thermal capacitances (cumulative thermal capacitance) in the function of the sum of the thermal resistances (cumulative thermal resistance) of the thermal system, measured from the point of excitation towards the ambient. Discretization of the structure function results in a Cauer network. The slight dip in the minimum junction temperature and the maximum junction temperature is as a result of the changes in the ambient.

The result of several measurements made during power cycling can be seen in Figs. 13 and 14. The differential structure function is represented in Fig. 13 with no noteworthy difference in the measurements performed. The best way of observing these measurements is by using the cumulative structure function. As mentioned earlier, discretization of the structure function leads to a Cauer network. Hence, picking a point on the thermal capacitance axis is the same as picking a point in the structure of the device and obtaining its thermal resistance. This cannot be directly implemented with the differential structure function. By using this process on the cumulative structure function measurements shown in Fig. 14 the degradation on the power module can be obtained in form of the thermal resistance with respect to time.

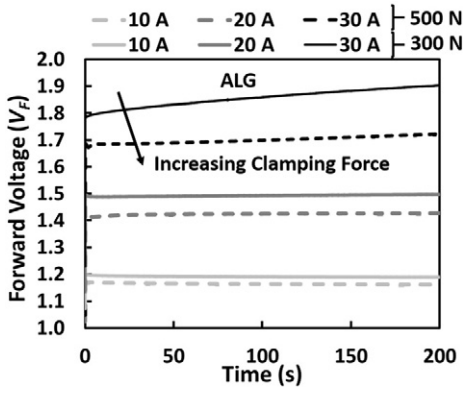

Fig. 8. Forward voltage during heating for ALG and different clamping forces ($F =$ 300 N and $F =$ 500 N).

Table 2
Analytical and measured thermal resistances.

Unit (K/W)	Analytical	Peaks
Die	0.2219	0.2489
Die + contact	1.0049	0.8908

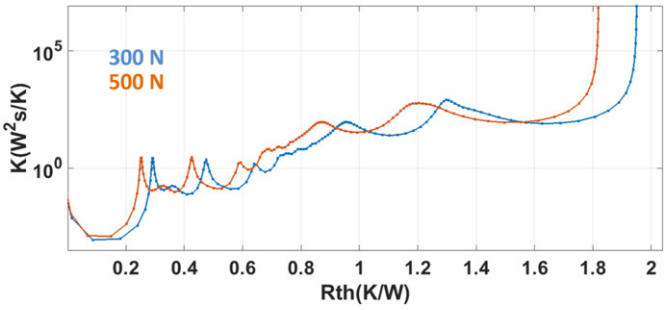

Fig. 11. Differential structure for ALG 500 N and 300 N.

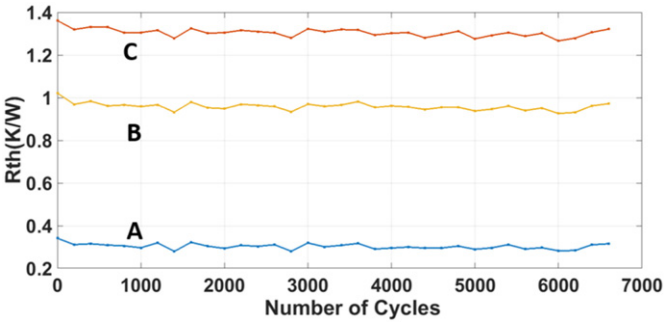

Fig. 15. Thermal impedance degradation plot.

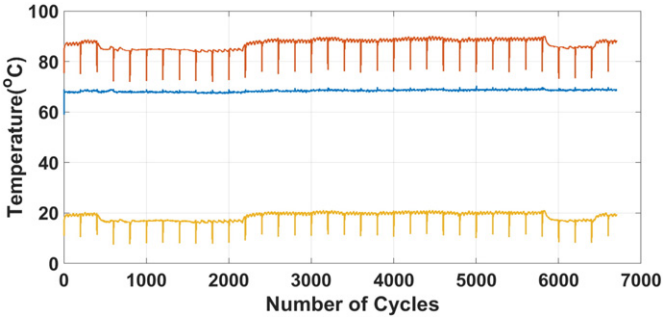

Fig. 12. Power cycling parameters: T_{Jmax} (red), T_{Jmin} (yellow) and ΔT_J (blue).

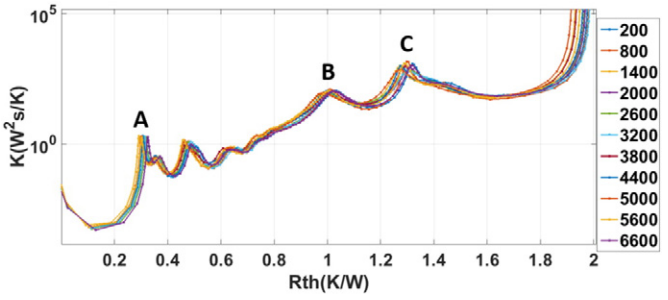

Fig. 13. Differential structure function for 6600 cycles.

Three points in the cumulative structure function have been chosen to check for degradation. These points correspond to the points on cumulative structure function where there is a change in capacitance which corresponds to the peaks in the differential structure function. It can be seen in Fig. 15 that at the different interfaces there is no noteworthy change in thermal resistance which means there is no degradation so far.

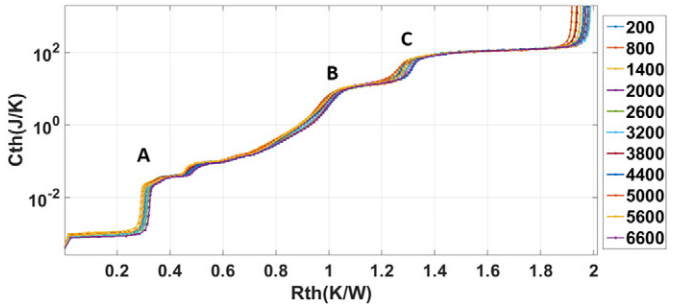

Fig. 14. Cumulative structure function for 6600 cycles.

5. Conclusions

It has been shown in this work that although ALG has higher electrical resistivity it also has a lower thermal resistance than molybdenum. It means that for the same power ALG press pack design can be smaller (by reducing the size of the heatsink for example), also by using higher clamping force the electrical resistance and thermal resistance can be reduced. The preliminary cycling tests show no degradation and are still ongoing. A different failure mechanism is expected due to the absence of solder, which is the predominant failure mode in SiC according to [1].

The future work entails the introduction of the solder layer between the die and the contact to reduce the contact resistance and thermal resistance. However that might have an effect on the reliability. Both an assembly with solder and no solder will be studied.

Acknowledgements

This work was supported by the UK Engineering and Physical Science Research Council (EPSRC) through the Underpinning Power Electronics Devices Theme (EP/L007010/1), Components Theme (EP/K034804/1) and HUB (EP/K035304/1).

References

[1] C. Herold, M. Schaefer, F. Sauerland, T. Poller, J. Lutz, O. Schilling, Power cycling capability of modules with SiC-diodes, Integrated Power Systems (CIPS), 2014 8th International Conference on, Nuremberg, Germany 2014, pp. 1–6.
[2] J. Lutz, et al., Semiconductor Power Devices - Physics, Characteristics, Reliability, Springer-Verlag, 2011.
[3] Y. Sugawara, S. Ogata, et al., 4.5 kV 1000 A class SiC pn diode modules with resin mold package and ceramic flat package, Power Semiconductor Devices and IC's, 2008, ISPSD '08. 20th International Symposium on, Vol., No., 18–22 May 2008, pp. 267–270.
[4] V. Banu, P. Godignon, X. Perpiñà, et al., Enhanced power cycling capability of SiC Schottky diodes using press pack contacts, Microelectron. Reliab. 52 (9–10) (September–October 2012) 2250–2255.
[5] Schunk Hoffmann Carbon Technology AG, www.hoffmann.at.
[6] P. Rajaguru, H. Lu, C. Bailey, J. Ortiz-Gonzalez, O. Alatise, Electro-thermo-mechanical modelling and analysis of the press pack diode in power electronics, Thermal Investigations of ICs and Systems (THERMINIC), 2015 21st International Workshop on, Paris 2015, pp. 1–6.
[7] C. Busca, R. Teodorescu, F. Blaabjerg, L. Helle, T. Abeyasekera, Dynamic thermal modelling and analysis of press-pack IGBTs both at component-level and chip-level, Industrial Electronics Society, IECON 2013 - 39th Annual Conference of the IEEE, Vienna 2013, pp. 677–682.
[8] M.M. Yovanovich, Four decades of research on thermal contact, gap, and joint resistance in microelectronics, IEEE Trans. Compon. Packag. Technol. 28 (2) (June 2005) 182–206.
[9] L.R. GopiReddy, L.M. Tolbert, B. Ozpineci, Power cycle testing of power switches: a literature survey, IEEE Trans. Power Electron. 30 (5) (May 2015) 2465–2473.
[10] www.mentor.com/products/mechanical/micred/t3ster.

[11] V. Székely, A new evaluation method of thermal transient measurement results, Microelectron. J. 28 (3) (1997) 277–292.
[12] V. Szekely, T. Van Bien, Fine structure of heat flow path in semiconductor devices: a measurement and identification method, Solid State Electron. (V.31) (1988) 1363–1368.
[13] M. Rencz, V. Szekely, Structure function evaluation of stacked dies, Semiconductor Thermal Measurement and Management Symposium, 2004, Twentieth Annual IEEE, 2004.